JOURNAL OF COLLOID AND INTERFACE SCIENCE **188,** 251–256 (1997)
ARTICLE NO. CS964745

Disaggregation of Particles with Biospecific Interactions in Shear Flow

ANDREI A. POTANIN,*,[1] VLADISLAV V. VERKHUSHA,†,[2] AND VLADIMIR M. MULLER‡,[3]

*Center for Materials for Information Technology, University of Alabama, Tuscaloosa, Alabama 35487; †Institute of Applied Research, Moscow State University, P.O. Box 20, Moscow 109035, Russia; and ‡Institute of Physical Chemistry, Russian Academy of Science, Russia

Received February 23, 1996; accepted December 16, 1996

The disaggregation of biospecifically interacting particles in shear flow is studied on the basis of kinetic modeling of formation and breakup of ligand–receptor bonds. The reaction rate theory is employed to improve earlier estimations of the critical force required to separate the surfaces. A chain of particles connected through ligand–receptor bonds responds to an external load as a contorted elastic rod. The breakup of the many-particle aggregate is attributed to the rupture of the backbone rod-like chain of particles. The theoretical model is found to be in good agreement with our experimental data on disaggregation of particles of latex immunoconjugates and blood platelets in shear flow.

1. INTRODUCTION

Shear flow often has a significant effect on aggregation–disaggregation processes in colloidal dispersions. In the early stages of aggregation shear flow promotes aggregation (1–3), while in the later stages it limits the aggregate growth (4–8). The maximum aggregate radius, R, decreases with the shear rate, S. Sometimes a power law is used, i.e.,

$$R \propto S^{-m} \qquad [1]$$

with the exponent, m, ranging in the limits 0.3–0.5.

In biological and biotechnological applications it is necessary to deal with a variety of interactions relevant to the aggregation–disaggregation of particles, in particular biological cells. Surfaces of particles or cell membranes are often connected by ligand–receptor bonds. These *biospecific* interactions are responsible for many important biological phenomena such as platelet aggregation. Earlier we presented a model for the doublet formation of biospecifically interacting particles in shear flow (2). In this work we focus on the modeling of the later stages of aggregation. A kinetic model of the ligand–receptor bond breakup is considered in Section 2. In Section 3 the breakup of multiparticle aggregates is considered. Finally we combine both models to describe our experimental data on disaggregation of latex immunoconjugates and blood platelets in Section 4.

2. KINETIC MODEL OF LIGAND–RECEPTOR BOND BREAKUP

Following (2) we consider the two-stage ligand–receptor interaction, which obeys the following scheme:

$$R + L \leftrightarrow R.\ .L \leftrightarrow RL. \qquad [2]$$

The corresponding kinetic equations read

$$\frac{\partial [R.\ .L]}{\partial t} = 2k_1[R][L] - (k_2 + k_3)[R.\ .L] + k_4[RL], \qquad [3]$$

$$\frac{\partial [RL]}{\partial t} = k_3[R.\ .L] - k_4[RL], \qquad [4]$$

$$[R]_0 = [R] + \frac{1}{2}[R.\ .L] + \frac{1}{2}[RL], \qquad [5]$$

$$[L]_0 = [L] + \frac{1}{2}[R.\ .L] + \frac{1}{2}[RL], \qquad [6]$$

where symbols R, L, $R.\ .L$, and RL designate disaggregated receptors and ligands, collision complexes formed in the first stage of reaction, and bound ligand–receptor complexes (LRC); square brackets designate corresponding surface concentrations; $[R]_0$ and $[L]_0$ are the total surface concentrations of receptors and ligands; and k_1, k_2, k_3, and k_4 are kinetic parameters which will be defined below. In what follows we assume $[L]_0 \ll [R]_0$ and set ligand and receptor radii equal to c, such that $c \ll \delta$, where δ is the length of

[1] To whom correspondence should be addressed at current address: Quantegy, Inc., P.O. Box 190, 2230 Marvyn Parkway, Opelika, Alabama 36803-01090.

[2] Current address: Kyoto Research Park, Tsukita ''Cell Axis'' ERATO Project, 17 Chudoji Minami-machi, Shimogyo-ku, Kyoto 600, Japan.

[3] Deceased December 23, 1995.

0021-9797/97 $25.00

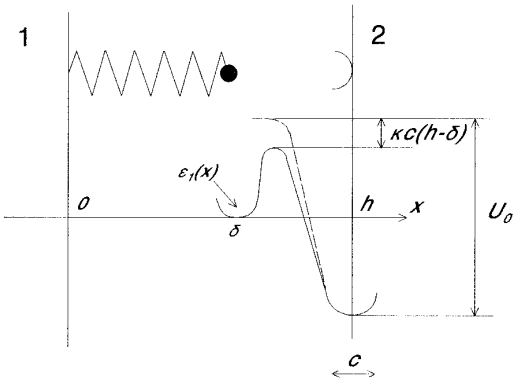

FIG. 1. Schematic of interaction of receptor on surface 2 with the coreceptor on surface 1. The latter consists of the ligand and spring-like molecular bond.

LRC (see Fig. 1). Kinetic parameters of the first reaction stage are

$$k_1 \sim D, \quad k_2 \sim D/c^2, \tag{7}$$

where $D = kT/6\pi\eta c$ is the diffusion coefficient and η is the viscosity of the liquid.

To estimate the kinetic parameters for the second reaction stage the ligand is considered a Brownian particle moving in the potential, $U(x)$, where x is the distance of the ligand from surface 1, to which it is bound by the polysaccharide molecule, while the receptor on surface 2 also attracts the ligand via some short-range potential, $U_{lr}(h - x)$, as shown in Fig. 1. The polysaccharide molecule is modeled as a Hookean spring with the force constant, κ, and equilibrium length, δ, i.e.,

$$U(x) = \epsilon_1(x) + U_{lr}(h - x), \tag{8}$$

where $\epsilon_1(x) \equiv \kappa(x - \delta)^2/2$. We assume that the potential, $U_{lr}(x)$, is characterized only by two parameters: the characteristic energy of interaction, U_0, and the width of the potential well, $\sim c$. Hence, the maximum of the potential barrier is found at point $x_b \sim h - c$, while the two equilibrium positions are at $x_0 = \delta$ and $x_0 = h$, which correspond to the $R\ldots L$ and RL states. The transition from one state to the other occurs whenever the ligand passes x_b. To estimate the transition time we employ reaction rate theory (9) and write

$$\tau(x_0) = \frac{2\pi}{\eta c}\sqrt{U''(x_b)U''(x_0)}\,\exp\frac{U(x_b) - U(x_0)}{kT}. \tag{9}$$

For the $R\ldots L \to RL$ transition the barrier height is estimated as

$$U(x_b) - U(\delta) = \kappa(h - \delta)^2/2, \tag{10}$$

while for the $RL \to R\ldots L$ transition the barrier is

$$U(x_b) - U(h) = U_0 - \kappa(h - \delta)c. \tag{11}$$

Second derivatives follow as

$$U''(\delta) \sim \epsilon''(\delta) = \kappa, U''(h) \sim U''(h - c) \sim U_0/c^2 \tag{12}$$

and the kinetic parameters are

$$k_3 = 1/t(\delta) \sim k_{30}e^{-(\kappa(h-\delta)^2)/kT},$$
$$k_4 \sim 1/t(h - c) \sim k_{40}e^{-(\kappa c(h-\delta))/kT}, \tag{13}$$

where

$$k_{30} \sim \frac{\sqrt{\kappa U_0}}{\eta c^2}, \quad k_{40} \sim \frac{U_0}{\eta c^3}\exp - \frac{U_0}{kT} \tag{14}$$

are their equilibrium values. Note that these estimations apply to the high-barrier case, namely

$$U_0 > \kappa c(h - \delta), \quad U_0 > kT. \tag{15}$$

Now we take into account that $[L]_0 \ll [R]_0$ and find from Eqs. [5] and [6] that

$$[R][L] \approx [R]_0[L]_0 - \frac{1}{2}([RL] + [R\ldots L]). \tag{16}$$

In equilibrium we find from Eq. [4]

$$[R\ldots L] = \frac{2[L]_0 + ((k_4 - k_1[R]_0)/k_1[R]_0)[RL]}{1 + ((k_2 + k_3)/k_1[R]_0)}. \tag{17}$$

Now we use Eq. [17] to exclude $[R\ldots L]$ from Eq. [4] and get

$$\frac{\partial[RL]}{\partial t} = -\left(k_4 + \frac{(k_1[R]_0 - k_4)k_3}{k_1[R]_0 + k_2 + k_3}\right)[RL]$$
$$+ \frac{2k_1k_3[R]_0}{k_1[R]_0 + k_2 + k_3}[L]_0. \tag{18}$$

Let us assume that the following conditions are satisfied:

$$k_1[R]_0k_2 \gg k_3, k_4. \tag{19}$$

These conditions imply that the first reaction stage, $R + L \leftrightarrow R\ldots L$, is considerably faster than the second,

$R. .L \leftrightarrow RL$. Since $c^2[R]_0 \gg 1$, we take into account Eqs. [7], [13], and [14] and rewrite Eq. [19] as

$$\frac{\kappa c^2}{kT}\frac{U_0}{kT} \ll 1, \qquad [20]$$

which means that the bond is not very strong. In this case Eqs. [4], [3], [5], and [6] are rewritten as

$$\frac{\partial[RL]}{\partial t} = -(\sigma k_3 + k_4)[RL] + 2\sigma k_3[L]_0, \qquad [21]$$

where $\sigma \equiv 1/[1 + (k_2/k_1[R]_0)]$ is a coefficient of order unity.

It is worthwhile to note that an equation similar to our Eq. [21] was postulated by Bell in (10). He assumed that k_4 depends upon the gapwidth h (or, in his notations, upon the external force $f \equiv \kappa(h - \delta)[RL]$) via exponential law similar to what we used in Eq. [13], but he set k_3 constant. Now if we take into account that k_3 also depends upon h or f as given by Eq. [13], we obtain a corrected Bell's equation,

$$\frac{2[L]_0}{k_4\xi}\frac{\partial\xi}{\partial t} = \Phi(\xi, u, w) \equiv K\frac{1-\xi}{\xi}\exp\left(-\frac{u}{\xi} - \frac{wu^2}{\xi^2}\right) - 1, \qquad [22]$$

where $\xi \equiv [RL]/2[L]_0$, $u \equiv cf/2[L]_0kT$, $w \equiv kT/2\kappa c^2$, and $K \equiv \sigma k_{30}/k_{40}$.

Let us now discuss the properties of Eq. [22] assuming $K \gg 1$, which is satisfied for all practical purposes. Under weak load, $u < u_c$ or ($f < f_c$), Eq. [22] has the stable point at $\xi = \xi_c$, while at $u > u_c$ (or $f > f_c$) the stable point disappears; i.e., bonds are irreversibly broken. Here u_c and f_c are critical values of u and f, which are found from the equations

$$\Phi(\xi_c, u_c, w) = 0, \quad \frac{\partial\Phi(\xi_c, u_c, w)}{\partial\xi} = 0. \qquad [23]$$

From Eq. [23] we find

$$u_c = \frac{\xi_c}{2w}\left\{-1 + \left[1 + 4w\ln\left(K\frac{1-\xi_c}{\xi_c}\right)\right]^{1/2}\right\}, \qquad [24]$$

$$\xi_c \equiv \frac{u_c - 2wu_c^2 + [(u_c - 2wu_c^2)^2 + 8wu_c^2(1 + u_c)]^{1/2}}{2(1 + u_c)}. \qquad [25]$$

Note that if

$$w\ln K \ll 1, \qquad [26]$$

then Eqs. [24] and [25] are reduced to that proposed by Bell (10):

$$u_c\exp[1 + u_c] = K. \qquad [27]$$

A simplified estimate of u_c up to a numerical coefficient can be obtained from Eq. [24] by setting in it ξ_c and $\ln(K(1 - \xi_c)/\xi_c)$ equal to 1:

$$u_c = \frac{1}{2w}\left\{-1 + \left[1 + 4w\ln K\right]^{1/2}\right\}. \qquad [28]$$

In the limiting case of [26] we get

$$u_c \approx \ln K, \quad \frac{f_c}{2[L]_0} \approx \frac{kT}{c}\ln K. \qquad [29]$$

A similar estimate (up to an insignificant coefficient 0.7) was obtained by Bell (10) from Eq. [27]. From our analysis we see that this estimate is actually incorrect, because the condition [26] contradicts the condition [20] of the applicability of this approach. It is worthwhile to note that in the opposite limiting case, $w \ln K \gg 1$, we find from [24]

$$u_c \approx \left(\frac{\ln K}{w}\right)^{1/2}, \quad \frac{f_c}{2[L]_0} \approx (kT\kappa\ln K)^{1/2}; \qquad [30]$$

i.e., the critical load turns out to be smaller than predicted by Bell's equation [29].

3. BREAKUP OF AGGREGATES

Let us now consider the breakup of aggregates in which particles are connected via LRC complexes. We consider spherical particles, which is the case for latexes, but this might seem a very strong assumption with respect to platelets. In fact, activated platelets have irregular shapes so that describing them as spheres should be understood as a very simple model for a complicated problem. Aggregates are assumed isotropic with the radius of gyration R_g.

The range of biospecific interactions is determined by the maximum length of LRC, L. Due to stretching of LRC under an external load, L can exceed the equilibrium length of LRC, δ, but we assume that polysaccharide molecules in LRC are rigid enough so that $|L - \delta| \ll \delta$. We also assume that $L \ll a$, where a is the radius of particles. Approximating spherical surfaces by parabolic ones, we write the local gap width, h, as

$$h = h_0 + \frac{r^2}{a}, \qquad [31]$$

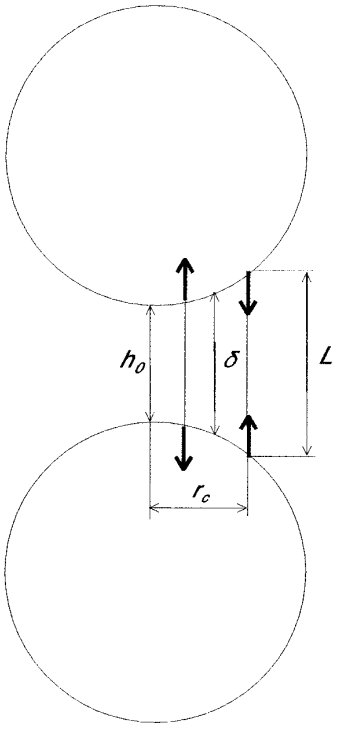

FIG. 2. Schematic of interaction of two particles.

where h_0 is the minimum gap width (see Fig. 2) and r is the radial coordinate. The LRC breakup dominates over their creation at $h > L$, where L is related to the energy, U_c, of the LRC breakup via the formula

$$\epsilon_1(L) \equiv \frac{1}{2}\kappa(L-\delta)^2 = U_c \sim \kappa c^2\left[1+\left(1+2\frac{kT}{\kappa c^2}\ln\frac{\sigma k_{30}}{k_{40}}\right)^{1/2}\right]. \quad [32]$$

The radius of the contact zone, r_c, defined in Fig. 2, is found as

$$r_c = \sqrt{a(L-h_0)}. \quad [33]$$

The surface density of LRC, n, is assumed close to $2[L]_0$, which corresponds to the case discussed in Section 2. Integrating the interaction force per unit area, $-nd\epsilon_1(h)/dh$, over the contact zone and equating the result to zero we find the following relation valid in equilibrium:

$$r_c = \sqrt{2a(L-\delta_0)} = \sqrt{2a\delta}\left(\frac{2U_c}{\kappa\delta^2}\right)^{1/4}. \quad [34]$$

Now let us consider a backbone chain of particles which spans the aggregate and holds it together. The end-to-end distance of the chain is on the order of the radius of gyration of the aggregate, R_g. Below we will assume that the chains are isotropic, so that the transverse size of the chain is also of order R_g. When external forces, $\pm\mathbf{F}$, are applied to the ends of the chain along its end-to-end vector, it will deform as an elastic rod. The bending moment is $\Gamma \sim FR_g$. The chain ruptures if Γ exceeds the critical value, $\Gamma_c \sim \kappa_1 n r_c^3 l$, where l is the critical elongation of LRC related to the critical energy, U_c^*, through $\epsilon(L+l) = U_c^*$. To estimate U_c^* we assume that the breakup is essentially activated by shear flow if the number of LRC ruptured during the period $\sim 1/S$ of aggregate rotation is of order nr_c^2, i.e., is comparable to the total number of LRC in the contact zone. Estimating the time required for rupture as $k_4^{-1} nr_c^2$ with $k_4 = k_{40}\exp(-U_c^*/kT)$ we obtain

$$\frac{U_c^*}{kT} \sim \ln(Snr_c^2/k_{40}). \quad [35]$$

Consider the aggregate as a sphere with hydrodynamic radius $\sim R_g$. In shear flow the force, $F \sim \eta S R_g^2$, is applied to each of the two hemispheres stretching the aggregate into pieces. The aggregate will be broken if $F > \Gamma_c/R_g$. From this the maximum size of aggregates which remain stable at given shear rate follows as

$$\frac{R_g}{a} = \left[\lambda n\delta^2\left(\frac{U_c}{\kappa\delta^2}\right)^{5/4}\left(\frac{\delta}{a}\right)^{5/2}\frac{\kappa}{\eta\delta S}\right]^{1/3}, \quad [36]$$

where the dimensionless parameter

$$\lambda \equiv \left(\frac{U_c^*}{U_c}\right)^{1/2} - 1 \sim \left\{\frac{kT\ln(Snr_c^2/k_{40})}{\kappa c^2[1+(1+2(kT/\kappa c^2)\ln(\sigma k_{30}/k_{40}))^{1/2}]}\right\}^{1/2} - 1 \quad [37]$$

characterizes the LRC breakup kinetics.

The applicability of our simplified kinetic model of LRC breakup is limited to sufficiently high shear, such that $U_c^* > U_c$ or $\lambda > 0$. The parameter λ is weakly dependent on S. To simplify the model even further λ can be set constant, in which case Eq. [36] predicts the scaling law [1] with $m = \frac{1}{3}$. Earlier several authors attempted to determine the exponent m. In particular, computer simulations were employed. Thus, Potanin (7) found $m = 0.4 - 0.5$ for a system with central force interactions, while for a system with bond-bending forces m was smaller, although no quantitative data were published. For a system of nonslipping spheres in 2D, Doi and Chen (8) found m close to our value $\frac{1}{3}$. However,

one should be careful in applying these simulation results to real systems because (i) hydrodynamic interactions were neglected and (ii) nonhydrodynamic interactions were treated in a somewhat oversimplified way.

4. EXPERIMENTAL

We studied aggregation in two systems: dispersions of human blood platelets and latex particles covered by antibodies, i.e., immunoconjugates. Our experimental setup is described in detail in (11). Basically, the shear flow is generated in the gap between two cylinders and the aggregation is characterized via turbometric measurements.

Aggregation of platelets was studied in platelet-rich blood plasma (PRP) after depletion of erythrocytes by means of centrifuging (11, 12). Platelet concentration in PRP was maintained at 4×10^6 cells/ml by dilution with platelet-free plasma. Aggregation of PRP in shear flow was initiated by addition of adenosine 5′-diphosphate (inducer of aggregation). The aggregation proceeds in three basic stages: (i) the cells become spherical due to the transformation of their internal cytoskeletal structure, enabling the receptors to bind to fibrinogen from plasma; (ii) receptor–fibrinogen complexes are formed and play the role of coreceptors (represented by a spring-like bond in Fig. 1); (iii) collisions of activated platelets in shear flow results in their aggregation through receptor–coreceptor interaction and finally in formation of doublets, triplets, and larger aggregates. Since the formation of receptor–fibrinogen complexes proceeds much slower than the collision rate of platelets (12), we assume $[R]_0 \ll [L]_0$ as stated above.

The aggregates were fixed by addition of 1% paraformaldehyde after the completion of aggregation, i.e., after stabilization of the turbometric data. After that we waited 10 min and gently transferred the aggregates to the microscope. The average aggregate radius was determined from a sampling of ~100 aggregates. It is worthwhile to note that the aggregates formed due to the breakup of cell membranes were excluded from consideration. Also excluded were single viable cells, which did not take part in aggregation due to their refractoriness (insensitivity) to the inducer of aggregation and therefore were incapable of binding fibrinogen. The average radius of platelets thus determined was 1.2 μm.

Immunoconjugates were formed by physical adsorption of polyclonal rabbit IgG antibodies to the polysaccharide (poly-3-*O*-acetyl-2-deoxy-α-mannosamine) of meningococcus serogroup A on the surface of polystyrene latex with consequent eluting of the nonadsorbed antibodies. The averaged radius of latex particles was 0.6 μm. The aggregation of immunoconjugates was initiated by adding the polysaccharide into the sheared suspension at a concentration of 10^{-9} *M*. The concentration of immunoconjugates in suspension was 10^7 particles/ml. Fixation and determination of the average radius of aggregates were performed in the same way as for blood platelets. Considering $[R]_0$ and $[L]_0$ as the surface concentrations of free antibodies and antibody–polysaccharide complexes, respectively, we again assume that $[R]_0 \ll [L]_0$.

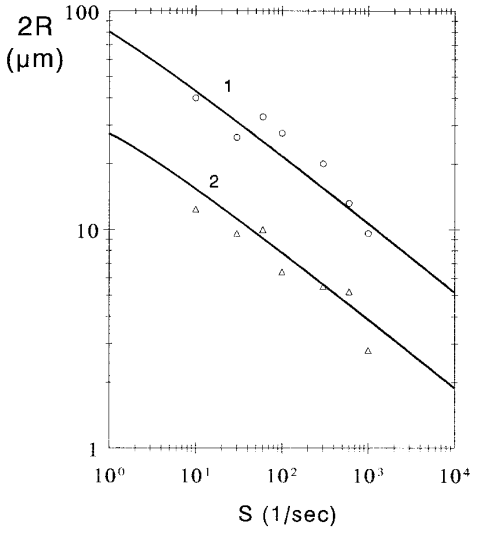

FIG. 3. Experimental data for platelets (1, ○) and latexes (2, △) are compared with theoretical calculations for aggregate diameter upon shear rate.

In Fig. 3 we plot the results of the experiments and the calculations according to Eq. [36] of the dependence of the aggregate diameter on the shear rate *S* for latex immunoconjugates ($a = 0.6$ nm, curve 1) and platelets ($a = 1.2$ nm, curve 2). The following parameters were used:

$$U_0 = 30kT, \quad \kappa = 10^{-4}\ \text{N/m}, \quad \delta = 10\ \text{nm}, \quad c = 1\ \text{nm}, \quad \sigma \sim 1. \quad [38]$$

We found our calculations in good agreement with the experimental data at $n\delta^2 = 1$ for latexes and $n\delta^2 = 7$ for platelets. The increased value of n for platelets can be attributed to the lateral diffusion of LRC, which results in accumulation of ligands in the contact zones. Obviously, lateral diffusion is not relevant to antibodies of latex immunoconjugates.

5. CONCLUSION

A model for the disaggregation of particles interacting via bridges of ligand–receptor complexes (LRC) which bind their surfaces has been presented. The model includes three stages. First, kinetic analyses were employed to estimate the specific energy required to separate bound surfaces. An earlier model of Bell (10) was improved. Second, the breakup of chains of particles connected via LRC was considered and the critical force that should be applied to the ends of the chain to cause its rupture was estimated. Finally, the

breakup of the spherical aggregate in shear flow was modeled, attributing it to the rupture of the backbone chain which holds the aggregate in one piece under the external hydrodynamic force. Thus the dependence of the aggregate size upon shear rate was found and compared with experimental data for blood platelets and latex immunoconjugates. The data are in good agreement with calculations at reasonable values of the parameters of LRC.

ACKNOWLEDGMENT

We gratefully acknowledge the support of the International Science Foundation (Soros Foundation), Project NCY000.

REFERENCES

1. Van de Ven, T. G. M., and Mason, S. G., *Colloid Polym. Sci.* **255,** 468 (1977).
2. Potanin, A. A., Verkhusha, V. V., and Vrzheshch, P. V., *J. Colloid Interface Sci.* **160,** 405 (1993).
3. Torres, F. E., Russel, W. B., and Schowalter, W. R., *J. Colloid Interface Sci.* **142,** 554 (1991); *J. Colloid Interface Sci.* **145,** 51 (1991).
4. Sonntag, R. C., and Russel, W. B., *J. Colloid Interface Sci.* **113,** 111 (1986); *J. Colloid Interface Sci.* **115,** 378 (1987).
5. Brakalov, L. B., *Chem. Eng. Sci.* **42,** 2373 (1987).
6. Peng, S. J., and Williams, R. A., *J. Colloid Interface Sci.* **166,** 321 (1994).
7. Potanin, A. A., *J. Colloid Interface Sci.* **157,** 399 (1993).
8. Doi, M., and Chen, D., *J. Chem. Phys.* **90,** 5271 (1989).
9. Hängi, P., Talkner, P., and Borkovec, M., *Rev. Mod. Phys.* **62,** 251 (1990).
10. Bell, G. I., *Science* **200,** 618 (1978).
11. Verkhusha, V. V., Lebedev, E. S., Vrzheshch, P. V., and Muller, V. M., *Colloid J. Rus. Acad. Sci.* **56,** 269 (1994).
12. Vrzheshch, P. V., Tatarintsev, A. V., Orlova, E. V., Yershov, D. E., and Varfolomeev, S. D., *Trombosis Res.* **67,** 505 (1992).